Available online at www.sciencedirect.com
SCIENCE DIRECT®
Journal of Controlled Release 96 (2004) 473–482
journal of controlled release
www.elsevier.com/locate/jconrel

Binding and detachment dynamics of microbubbles targeted to P-selectin under controlled shear flow

Amol M. Takalkar[a], Alexander L. Klibanov[a,b], Joshua J. Rychak[a], Jonathan R. Lindner[b], Klaus Ley[a,*]

[a] *Cardiovascular Research Center and Department of Biomedical Engineering, USA*
[b] *Cardiovascular Division, Department of Internal Medicine, University of Virginia, USA*

Received 21 October 2003; accepted 3 March 2004

Abstract

This study was performed to assess the binding kinetics of a targeted microbubble contrast agent exposed to shear stress. An ultrasound contrast targeted to P-selectin was designed by conjugating monoclonal antibodies against murine P-selectin (RB40.34) to the lipid monolayer shell of the microbubble using poly(ethylene glycol)-biotin–streptavidin. The attachment and detachment of targeted microbubbles to P-selectin immobilized on a culture dish were assessed in a parallel-plate flow chamber. Targeted microbubbles (5×10^6 particles/ml) drawn through the flow chamber coated with P-selectin (109 sites/μm^2) at a shear stress of 0.3 dyn/cm^2 accumulated at a rate of 565 mm^{-2} min^{-1}. Attachment rates increased at higher plate surface densities of P-selectin, and microbubble detachment was reduced. Accumulation rate first increased with shear stress, reached a maximum at $\sim$ 0.6 dyn/cm^2 and then decreased. Control experiments on a plate that lacked P-selectin, or was blocked with mAb RB40.34, resulted in minimal bubble attachment. Microbubble detachment was tested by ramping up shear stress at 30-s intervals. Half-maximal detachment was reached at 34 dyn/cm^2. Overall, accumulation and retention of targeted ultrasound contrast agents is possible under physiologic flow conditions and is strongly influenced by shear stress and surface density of the target receptor.

Keywords: Ultrasound contrast; Targeting; Microbubbles; Adhesion; P-selectin

1. Introduction

Ultrasound contrast agents composed of gas-filled microbubbles with diameters generally less than 5 μm have been in clinical use for several years [1–4]. These agents can improve the accuracy of assessing left ventricular function during echocardiography and allow imaging of tissue perfusion. The past few years have seen the development of site-targeted microbubbles that can be used for molecular and cellular imaging in vivo [5–8], as well as for ultrasound-assisted drug and gene delivery and triggered release [9–11].

One strategy to prepare targeted microbubbles is by coupling ligands specific to target receptors onto the

* Corresponding author. Cardiovascular Research Center, University of Virginia Health System, MR5 Bldg.-Rm. 1013 P.O. Box 801394 Charlottesville, VA 22908-1394, USA. Tel.: +1-434-243-9966; fax: +1-434-924-2828.
E-mail address: klausley@virginia.edu (K. Ley).

0168-3659/$ - see front matter © 2004 Elsevier B.V. All rights reserved.
doi:10.1016/j.jconrel.2004.03.002

microbubble surface. Such site targeted microbubbles bind to specific receptors expressed on cell surfaces and are thereby retained in the tissue. Adhesion behavior of these targeted microbubbles has been studied in a flow environment in vitro [12–14], but the dynamics of adhesion and detachment have not been fully characterized. The adhesion of leukocytes to endothelial cells has been extensively studied in vivo as well as in vitro. Parallel plate flow chamber systems have been used to study the adhesion of neutrophils [15], polystyrene beads [16,17] and nanospheres [18] to specific receptors on the target surface under static and flow conditions. Attachment of cells and beads depends on the site density of the adhesion molecules and on the fluid shear stress applied.

In this study, a parallel plate flow chamber system was applied to gain insights into the adhesion of targeted microbubbles to immobilized substrates. A system was developed and optimized to perform flow studies using targeted microbubbles with a commercially available parallel plate flow chamber by video microscopy. This study was undertaken to establish whether monoclonal antibodies against murine P-selectin attached to gas-filled microbubbles would bind to immobilized murine P-selectin under controlled shear conditions. Another reason for the study was to ascertain optimal site densities to promote maximal attachment rates and resistance to detachment. Understanding the process of targeted microbubble attachment and detachment may help in the prediction of in vivo behavior of targeted microbubbles and in the design of successful targeted preparations.

2. Materials and methods

2.1. Biotinylation of antibody

Monoclonal antibody (mAb) RB40.34 (Lymphocyte Culture Center, University of Virginia, Charlottesville, VA), a rat anti-mouse monoclonal IgG1 against murine P-selectin [19] was dialyzed overnight in phosphate buffered saline (PBS, Gibco Invitrogen, Grand Island, NY) using Slide-A-Lyzer 10 K dialysis cassettes (Pierce, Rockford, IL). Biotin *N*-hydroxysuccinimide ester (Sigma, St. Louis, MO) was used to biotinylate RB40.34 in PBS according to standard procedures [20]; unreacted biotin and reaction byproducts were removed by overnight dialysis in PBS. The amount of biotin on the antibody was determined using avidin-HABA (2-(4′ -hydroxyazonbenzene)benzoic acid, Pierce) displacement method [21]. There were approximately 0.37 to 0.9 mol of biotin per mol of biotinylated RB40.34 for various preparations.

2.2. Preparation of P-selectin substrates

Culture dishes (35 mm, Corning, Corning, NY) were rinsed with methanol and dried. PBS droplets (200 μl) containing dilutions (2.5–350 ng) of recombinant mouse P-selectin/Fc chimera (R&D Systems, Minneapolis, MN) were placed in a 1 cm diameter circular area on the dishes. The dishes were incubated overnight at 4 °C. The dishes were washed with PBS containing 0.05% Tween 20 (J.T. Baker, Phillipsburg, NJ) (PBS-Tween) and blocked with 2 ml of blocker casein solution in TBS (Pierce) for 1 h at room temperature.

2.3. P-selectin site density determination

Site densities of P-selectin on the polystyrene dishes were determined using time-resolved fluorescence detection of Eu-labeled streptavidin [22] (PerkinElmer Wallac, Turku, Finland). One milliliter of PBS containing 0.94 μg biotinylated RB40.34 was added to each P-selectin-coated dish, incubated at room temperature for 30 min and the unbound antibody was removed by six washes with PBS-Tween. One milliliter of 0.1 μg/ml Eu-labeled streptavidin solution was added to each plate and incubated at room temperature for 30 min. The dishes were washed with PBS-Tween, then 900 μl DELFIA enhancement solution (PerkinElmer Wallac) was added to each plate and incubated at room temperature for 5 min. Enhancement solution containing desorbed Eu was collected from each plate and placed in 96-well plates (300 μl per well). Time-resolved fluorescence was then measured using a SPECTRAmax Gemini XS dual-scanning microplate spectrofluorometer (Molecular Devices, Sunnyvale, CA) at 360 nm excitation and 610 nm emission. Fluorescence detection interval was 250–1250 μs. Control culture dishes with no P-selectin coat, blocked with casein in TBS were sim-

ilarly treated to obtain nonspecific background. Background-subtracted fluorescence counts were compared with a calibration curve for Eu-labeled streptavidin to obtain amount of Eu-labeled streptavidin on the culture dish. Surface site density of P-selectin was then calculated assuming 1:1 binding of P-selectin with RB40.34 as well as of RB40.34 with Eu-labeled streptavidin.

2.4. Preparation of targeted microbubbles

Microbubbles with monoclonal antibodies against P-selectin (MB_P) conjugated to their surface were designed as previously described [7]. Briefly, biotinylated microbubbles containing decafluorobutane gas (Flura, Newport, TN) were prepared by sonic dispersion of gas in the aqueous medium containing phosphatidylcholine, PEG stearate and biotin–PEG–DSPE; centrifugal flotation was applied to remove unincorporated lipids from microbubbles [23]. One milliliter of degassed PBS was added to 1 ml of biotinylated microbubbles and centrifuged at $400 \times g$ in a bucket rotor (HN-SII centrifuge, IEC, Needham Heights, MA). The floating density of gas-filled bubbles is effectively close to zero if compared with the density of the aqueous medium. Perfluorocarbon gas density is on the order of 0.01, and the shell contributes minimally to the bubble mass and volume; therefore, microbubble centrifugal flotation is a rapid and efficient process. The infranatant was drained and 2 ml of PBS was added to the supernatant cake of microbubbles. This process of washing the biotinylated microbubbles was repeated six times. They were then incubated on ice with 3 μg streptavidin (Sigma) for every 1×10^7 microbubbles for 30 min and washed twice. The streptavidin coated biotinylated microbubbles were then incubated on ice with 7.5 μg biotinylated RB40.34 for every 1×10^7 microbubbles for 30 min and again washed twice. Targeted microbubbles were thus prepared with biotinylated RB40.34 coupled to the phospholipid monolayer of the microbubble shell through a biotin–streptavidin bridge (Fig. 1). A Coulter Multisizer IIe (Beckman Coulter, Hialeah, FL) was used to determine the microbubble concentration, size distribution and surface area.

2.5. Measurement of antibody concentration on microbubble surface

Biotinylated RB40.34 was labeled with fluorescein isothiocyanate (FITC) (Sigma). Microbubbles targeted to P-selectin were prepared as described above using the FITC labeled antibody and the washes after incubating with the antibody were collected. Microbubble concentration and surface area were determined using a Coulter counter. The microbubbles were then destroyed by immersing the tube containing microbubble dispersion in an ultrasound bath (model

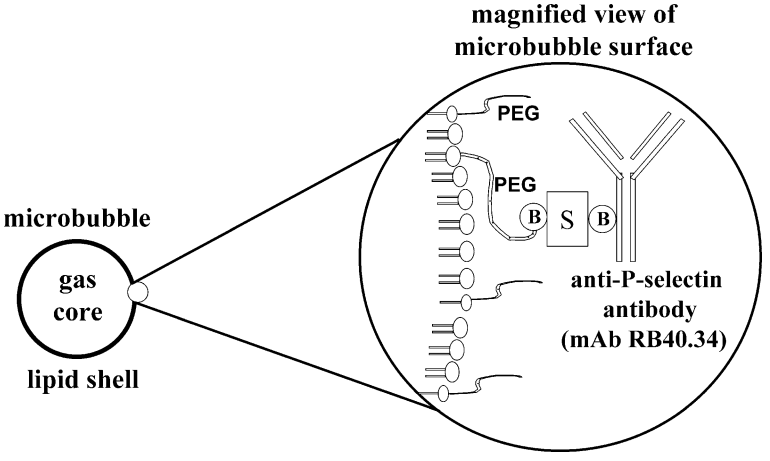

Fig. 1. Design of a targeted microbubble. A biotinylated monoclonal antibody (RB40.34) is coupled to the lipid monolayer of the microbubble using lipid–PEG–biotin (B) and streptavidin (S) spacer.

G112SP1T, Laboratory Supplies, Hicksville, NY) and fluorescence of the microbubble-derived samples as well as the wash infranatants was measured with a SPECTRAmax Gemini XS spectrofluorometer using 485 nm excitation and 538 nm emission settings. The amount of antibody on the microbubble surface was then calculated from the fluorescence present in the preparation of destroyed microbubbles, the amount and fluorescence of the antibody initially added, and the microbubble concentration data.

2.6. Flow chamber studies

The attachment and detachment studies were carried out using a parallel plate flow chamber [24,25] (Glycotech, Rockville, MD). The flow chamber was positioned in the custom-built stage adapter that inverted the chamber upside down. This geometry allowed microbubbles to float to and interact with the target surface during transit. Microbubbles (5×10^6 ml^{-1}) were drawn through the flow chamber using an adjustable infusion-withdrawal pump (Harvard Apparatus, Holliston, MA). Flow chamber width was 2.5 mm; chamber gasket thickness was 0.254 mm (0.01 in.). The pump flow rate was adjusted to obtain the desired shear stress at the substrate fluid interface, microbubble infusion initiated, and particle counting was started after a short delay necessary for the stabilization of the microbubble flux through the chamber. Video microscopy of microbubbles adhered to the upper deck of the flow chamber was performed using a 40× objective and a standard CCD camera attached to a Leitz Laborlux 11 microscope. The video was recorded onto Sony mini-DV tape using a Sony DSR-30 Digital VCR connected to the CCD camera and analyzed offline.

2.7. Microbubble accumulation on the target

MB_P (5×10^6 ml^{-1}) were drawn through the flow chamber at a shear stress of 0.3 dyn/cm^2 for 7 min. Their adhesion to the target surface with different P-selectin site densities (mean of 109, 7, or 3 molecules/μm) was assessed. The accumulation of MB_P at the shear stresses of 0.2, 0.3, 0.6, 1.0, and 1.7 dyn/cm^2 with the P-selectin site density of 109 molecules/μm^2 was also assessed. Control experiments were performed with plates with no P-selectin and on P-selectin coated plates blocked with excess RB40.34 prior to infusion of microbubbles. Quantitative analysis of microbubble accumulation was performed by counting the number of microbubbles adhered in the observed area at 60-s intervals and a graph of microbubble accumulation with time was plotted. The observation area was measured as 110 × 150 μm with the aid of a stage micrometer. Imaging was performed in the middle two-thirds of the flow deck.

2.8. Microbubble detachment from the target

Microbubbles were drawn into the flow chamber and allowed to interact with the target surface by flotation at zero flow for 2 min. After 2 min, PBS was drawn through the flow chamber at a shear stress of 0.15 dyn/cm^2 to remove stationary but not adhered microbubbles. The total number of microbubbles adhered was recorded and microbubble detachment was then assessed by drawing PBS through the flow chamber with incremental shear stress increases every 30 s.

3. Results

3.1. Biotinylated antibody

Binding of biotinylated RB40.34 to P-selectin was compared with that of normal RB40.34 to P-selectin

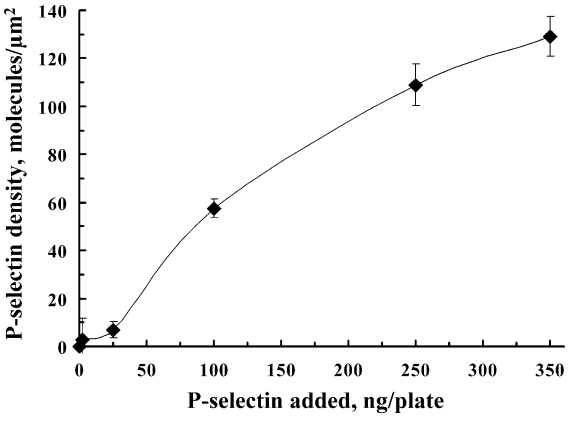

Fig. 2. P-selectin site density adsorption isotherm. Graph shows the P-selectin site density dependence on P-selectin concentration of the solution used for coating the culture dish. Data points taken in triplicate (mean ± S.E.M.).

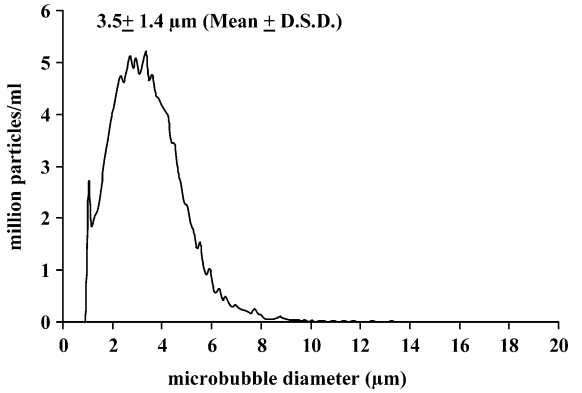

Fig. 3. Size distribution of MB_P targeted microbubbles (typical Coulter counter number distribution measurement presented).

using an ELISA technique. The biotinylated RB40.34 was found to possess somewhat decreased affinity to P-selectin, but sufficiently high for successful binding to the target (data not shown).

3.2. Characterization of P-selectin target surface

Surface site density of P-selectin was determined to be 109 ± 10 molecules/μm^2 (mean $\pm$ S.E.M.) when 250 ng of P-selectin solution was added onto the culture dish, 7 ± 4 molecules/μm^2 when 25 ng was added and 3 ± 9 molecules/μm^2 when 2.5 ng was added (see Fig. 2).

3.3. Characterization of targeted microbubbles

Fig. 3 shows the size distribution of a typical antibody-coated microbubble preparation. Mean microbubble diameter was ~ 3.5 µm. The size distribution profile did not show significant aggregation of microbubbles following the addition of streptavidin and biotinylated antibody (data not shown). The number of antibody molecules per microbubble was calculated to be $(102 \pm 3) \times 10^3$, or ~ 2500 RB40.34 antibody molecules per μm^2 of the microbubble surface. This translates to ~ 1 RB40.34 molecule for every 400 nm^2 (20×20 nm area, see Fig. 4).

3.4. Characterization of microbubble accumulation

Microbubble accumulation was studied under several sets of flow and antigen surface density conditions. Dishes with the antigen attached were post-blocked with casein solution to avoid nonspecific attachment of microbubbles. In several experiments, bovine serum albumin solution was used for blocking instead of casein and similar microbubble targeting behavior was observed. Keeping the shear

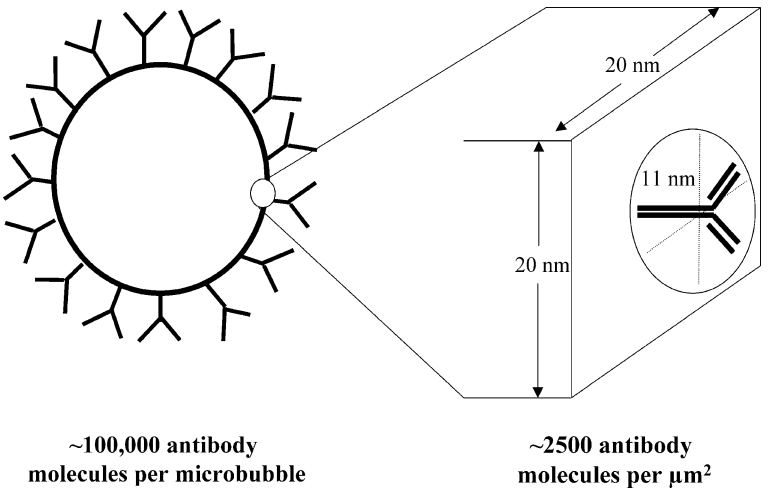

Fig. 4. From microbubble size distribution, the overall surface was calculated assuming spherical geometry, resulting in antibody surface density of ~ 2500 mAb molecules/um^2. A 20×20 nm membrane patch of the microbubble surface holds one molecule of RB40.34 on it. The hydrodynamic radius of an IgG antibody is about 5.5 nm.

stress and microbubble concentration constant at 0.3 dyn/cm^2 and 5×10^{-6} ml^{-1}, respectively, the microbubble accumulation over a 7-min interval at three P-selectin site densities was assessed (Fig. 5). Increased numbers of microbubbles accumulated at higher P-selectin site density and the difference in the accumulation rates (as computed by linear regression) was found to be statistically significant. Control experiments performed on culture dishes without any P-selectin or on culture dishes coated with P-selectin but blocked with excess mAb RB40.34 (Fig. 5, two lines on the bottom) demonstrated minimal accumulation of microbubbles compared to that when P-selectin was present on the culture dish.

3.5. Shear stress dependence

Microbubble accumulation was also assessed at five different shear stresses keeping the P-selectin site density at 109 molecules/μm^2 (Fig. 6). Linear regression analysis of the data sets was performed to assess the kinetics of microbubble accumulation on the target surface. Microbubble accumulation rate was found to be the greatest at a shear stress of 0.6 dyn/cm^2 as compared to the other shear stresses of 0.2, 0.3, 1 and 1.7 dyn/cm^2 (Figs. 6 and 7). The slopes of the linear regression lines in Fig. 6 represent the rate of microbubble accumulation per minute in the field of view.

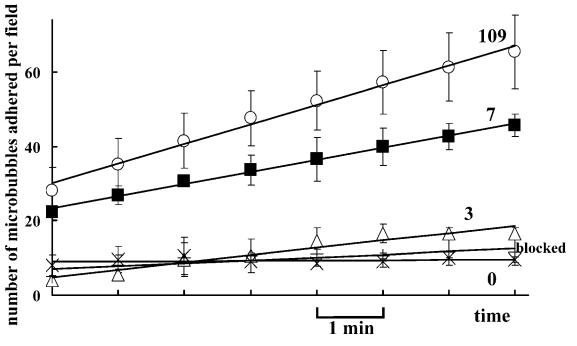

Fig. 5. Microbubble accumulation as a function of P-selectin site densities (109, 7 and 3 molecules/μm^2). Mean ± S.E.M., $n = 7$, 3, and 3, respectively. When P-selectin-coated surface (initially 109 molecules/μm^2 setting) was pre-blocked by incubation with excess soluble mAb RB40.34, attachment observed was similar to 0 site density (nonspecific, no P-selectin added).

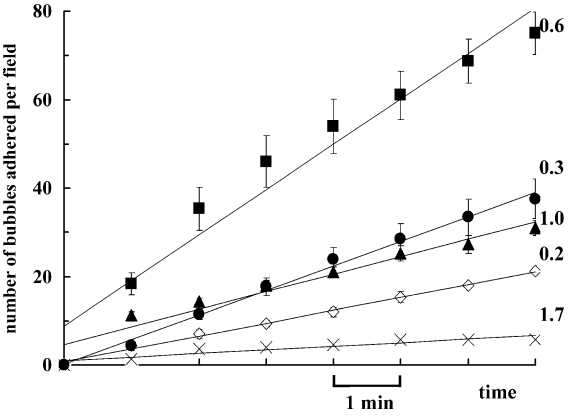

Fig. 6. Microbubble accumulation as a function of shear stress (0.2, 0.3, 0.6, 1 and 1.7 dyn/cm^2) at a P-selectin site density of 109 molecules/μm^2. Mean ± S.E.M., $n = 3$ for all curves.

The mean size of the bubbles accumulated on the P-selectin surface at 0.6 dyn/cm^2 shear as determined by video microscopy (~ 3.4 um) was similar to the mean size of the original microbubble dispersion preparation. The microbubble accumulation is low at higher shear stresses, increases as the shear stress decreases, reaches a peak and falls again at very low shear stresses. This behavior reflects the net balance between increased delivery at higher flow rates and decreased attachment at higher shear stress.

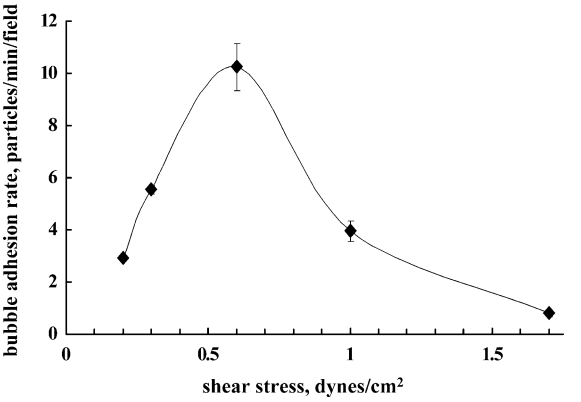

Fig. 7. Attachment rate as function of shear stress. Microbubbles attaching per 40 × field per min at various shear stresses. P-selectin site density was 109 molecules/μm^2. Maximal microbubble retention on the target occurs around a shear stress of 0.6 dyn/cm^2. (Statistically different from other flow rates, $p < 0.05$).

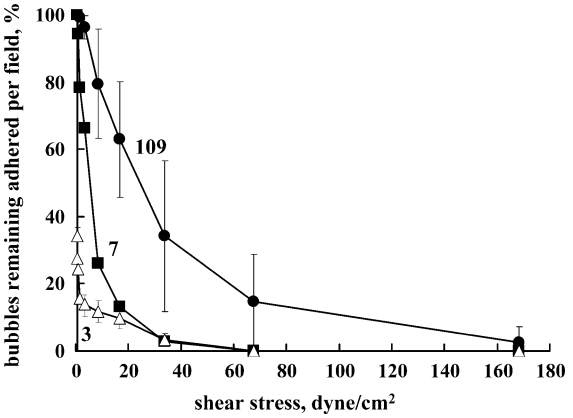

Fig. 8. Microbubble detachment resulting from periodic (every 30 s) incremental increases of the shear stress at P-selectin site densities of 109, 7 and 3 molecules/μm^2.

3.6. Characterization of microbubble detachment

Microbubble detachment was assessed by increasing the flow every 30 s and observing the number of microbubbles remaining bound. Fig. 8 shows the percentage of microbubbles remaining adhered to the target surface coated with three different P-selectin site densities. Better retention of microbubbles was found on the target surfaces with higher P-selectin site densities. For a P-selectin site density of 109 molecules/μm^2, half-maximal detachment was achieved at a shear stress of 34 dyn/cm^2.

4. Discussion

In this report, a rigorous quantitative analysis of the attachment and detachment properties of targeted microbubbles is provided. The salient findings include a monotonous increase of the rate of accumulation with P-selectin site density on the substrate and a bell-shaped dependence on wall shear stress with a maximum at 0.6 dyn/cm^2. This general behavior is similar to that of coated polystyrene beads on endothelial cells [17] or in a cell-free system [16]. Although the rate of attachment at 1.7 dyn/cm^2 and above was small, the targeted microbubbles could easily support continued adhesion once attachment had been achieved at this and higher wall shear stresses up to 65 dyn/cm^2 or more.

These findings have direct implications for strategies aimed at optimizing the local accumulation of targeted ultrasound contrast agents. Although one-step antibody-based systems like the one used here have successfully been used to delineate areas of inflammation in vivo by binding to the walls of post-capillary venules [7], this design is unlikely to provide attachment rates at high wall shear stress. However, the present data demonstrate that successful targeting may be possible in high-flow areas if a period of low flow can be achieved. Such situations can occur during organ transplantation, for example, of the kidney. Microbubbles targeted to P-selectin infused during an in vitro perfusion period conducted at reduced flow rates would likely be suitable to outline areas of inflammation and make them visible to ultrasound. It is known that the outcome of kidney transplantations is critically affected by the inflammatory response secondary to ischemia–reperfusion damage [26].

Effective attachment at high wall shear stresses is necessary to image sites of vascular inflammation in large vessels like inflamed atherosclerotic plaques (“vulnerable plaques”) in the carotid artery, coronaries, and the aorta. To achieve this, incorporation of selectin ligands on the microbubble surface may be required in addition to the targeting antibody. One such ligand, PSGL-1, has previously been shown to support attachment and slow rolling of beads up to shear stresses of 0.7 and 3.5 dyn/cm^2, respectively [16]. The selectin bond with this ligand is characterized by exceptionally high on-rates, much higher than the on-rates of antibody–antigen pairs [27,28], although the affinities of selectin ligand–selectin bonds fall within the same range as those of antibody–antigen bonds [27,28]. Consistent with antibody–antigen bond kinetics, microbubble rolling was not observed in this study at the shear stresses tested, presumably because the antigen–antibody bond, once formed, does not easily dissociate. This is also supported by the observation that targeted microbubbles, once allowed to attach to the target, remained stably bound even at very high levels of wall shear stress. Some of the previous studies using targeted nanospheres [18] also did not report rolling, but immediate arrest. In cell-based attachment systems, surface structures like extendable microvilli may also contribute to rolling phenomenon [29]. It is unlikely that for a

simple spherical microbubble antibody-mediated targeting the observed binding shear dependence (Fig. 7) with the maximum at 0.6 dyn/cm^2 could be caused by the complicated phenomena such as shear thresholding [30]. Shear thresholding was reported for PSGL-1-type ligands, and not for antibody-mediated adhesion so far. In case of antibody-mediated microbubble targeting, the microbubble target accumulation rates at shear stresses <0.6 dyn/cm^2 are nearly proportional to the flow rates and microbubble flux through the target area; at higher flow rates, the generated wall shear stress is sufficient to overcome the forces that retain the majority of the microbubbles on the target, and the rate of microbubble accumulation is reduced. The sum of these two effects causes a bell-shaped dependence of attachment rate on shear stress.

Previous reports have shown that targeted microbubbles can bind to cultured endothelial cells under flow conditions [12,14] and to post-capillary venules in the mouse cremaster muscle [7]. The levels of wall shear stress found in those systems are in the same general range (<2 dyn/cm^2), although higher shear stresses are found in some post-capillary venules [31]. It is possible that presentation of the target molecule on a cell rather than on plastic may be beneficial for delivery at higher wall shear stress. It was reported that microbubbles targeted to P-selectin bind through at least three mechanisms, binding to P-selectin expressed on the endothelium or on platelets, which in turn can bind to leukocytes, and binding to leukocytes through P-selectin independent processes [7]. Indirect microbubble delivery through platelet binding may enable even antibody-coated microbubbles to be delivered in areas of higher wall shear stress. However, a rigorous, complete characterization of microbubble binding and detachment kinetics is not possible in vivo because the local site density of the targeted molecule is unknown.

The measurement of surface site densities of P-selectin on the flow chamber plastic and of mAb RB40.34 on the microbubbles rests on several assumptions. Although this is true of all reported measurements of site densities, these assumptions are not always addressed explicitly. An assumption is made that one P-selectin molecule binds one antibody molecule, and each biotinylated antibody binds one Europium-labeled streptavidin. Since the level of biotinylation is less than 1 mol of biotin per mol of antibody, this appears reasonable, but direct proof that all the assumptions are met is not provided. For example, some P-selectin-IgG may be adsorbed to the plastic in an orientation that precludes antibody binding. Such a molecule would not be measured, but would also not be available to support targeted microbubble binding. The measured site density most likely represents a ''functional'' site density. The method reported here is an improvement over previous site density measurements [15] in that site densities are measured on the same tissue culture dish material as that used in the flow chamber. Site densities measured in a 48-well plate [15] may not exactly correspond to those in the flow chamber, even if concentration, time and temperature are matched, because the site density is likely influenced by the geometry, i.e. surface-to-volume ratio, and by the chemical composition of the polystyrene. Consistent with previous reports [32], a strongly nonlinear relation between the coating concentration and the resulting site density was found in this study.

Targeted microbubbles investigated in this study were prepared from water-insoluble decafluorobutane gas and stabilized with a monolayer of phospholipid, decorated with a brush of poly(ethylene glycol). A fraction of poly(ethylene glycol) chains carried biotin on the distal end of the polymer chain [23]. Such design allows attachment of a wide variety of biotinylated ligands, including antibodies, to the bubble surface via a streptavidin linker. While this targeted microbubble design is not directly applicable to the contrast agents for the use in patient studies, it offers flexibility, ease of use and reproducibility, desirable for the laboratory investigations. The average number of antibody molecules per bubble in the preparation studied is not very high, $\sim 10^5$, which is less than full coverage. The number of lipid molecules in a monolayer covering such an average bubble with a spherical shape and surface area of ~ 40 μm^2 can be computed as $\sim 8\times 10^7$. These 10^5 ligand molecules allow selective and reasonably firm binding to the target; the concentration of mAb RB40.34 on the microbubble surface is higher than the surface concentration of selectin ligands on cells (approximately 25,000 molecules PSGL-1 per leukocyte, [27]). Due to the difference in the particle size and surface area, ligand surface density difference between the bubbles and leukocytes is even more striking. Similar esti-

mates of antibody density on microbubbles were obtained earlier by an indirect FACS method [7]. Calculation of microbubble surface and antibody concentration in the preparations shows that there is on average one molecule of RB40.34 antibody per 20×20 nm microbubble surface area. The hydrodynamic radius of an IgG antibody is ~ 5.5 nm [33]. While this surface density does not amount to a geometrically complete coverage, ligand brought in contact with the microbubble has a high probability of a productive binding with antibody.

Future clinical usage of targeted ultrasound contrast agents will include selective imaging of the areas of inflammation, ischemia–reperfusion injury, angiogenesis and apoptosis, in large vessels or on the microvascular level, including the areas of rapid blood flow and high wall shear stress. In all of these conditions of interest, shear flow forces dominate buoyancy forces. Microbubbles have been reported to travel freely throughout the vasculature with the hydrodynamic behavior similar to red blood cells [34]. A typical imaging session lasts for 10–20 min after contrast administration; microbubble contrast is gradually cleared from the bloodstream and accumulated in the target area during this period, therefore, the timing interval chosen for this study is relevant for in vivo situations [7]. The microbubble preparations used in this study possess good in vivo stability and should be able to survive in vivo for tens of minutes, especially when attached to the target.

In conclusion, microbubbles targeted to P-selectin show optimal attachment at 0.5–1 dyn/cm^2, which is suitable for targeting to post-capillary venules of inflamed tissues in vivo. The considerable resistance to detachment even at very high wall shear stress suggests that targeted microbubbles can be designed for imaging of high-flow areas including vulnerable plaques in conduit arteries.

Acknowledgements

This work was supported by NIH BRP HL 64381 and a research grant from the Whitaker Foundation to K. Ley. J.J. Rychak is supported via NIH training grant HL07284. Generous donation of laboratory equipment to A.L. Klibanov's laboratory at UVA Cardiovascular Imaging Center by Mallinckrodt (St. Louis, MO) is appreciated. A.L. Klibanov is supported in part via DOE 43-14702, NIH DK63508 and HL64381. J.R. Lindner is supported in part via NIH DK63508, HL64381 and Grant-in-Aid GF10013 from the Atlantic Coast Affiliate of American Heart Association, Baltimore MD. A grant from the EIF Foundation to UVA Cardiovascular Division is gratefully acknowledged.

References

[1] S. Kaul, Myocardial contrast echocardiography: basic principles, Prog. Cardiovasc. Dis. 44 (1) (2001) 1–11.
[2] J.R. Lindner, K. Wei, S. Kaul, Imaging of myocardial perfusion with SonoVue in patients with prior myocardial infarction, Echocardiography 16 (7 pt 2) (1999) 753–760.
[3] D.M. Skyba, G. Camarano, N.C. Goodman, R.J. Price, T.C. Skalak, S. Kaul, Hemodynamic characteristics, myocardial kinetics and microvascular rheology of FS-069, a second generation echocardiographic contrast agent capable of producing myocardial opacification from a venous injection, J. Am. Coll. Cardiol. 28 (5) (1996) 1292–1300.
[4] M.A. Vannan, B. Kuersten, Imaging techniques for the myocardial contrast echocardiography, Eur. J. Echocardiog. 1 (3) (2000) 224–226.
[5] J.P. Christiansen, H. Leong-Poi, A.L. Klibanov, S. Kaul, J.R. Lindner, Noninvasive imaging of myocardial reperfusion injury using leukocyte-targeted contrast echocardiography, Circulation 105 (15) (2002) 1764–1767.
[6] J.R. Lindner, J. Song, A.L. Klibanov, K. Singbartl, K. Ley, S. Kaul, Noninvasive ultrasound imaging of inflammation using microbubbles targeted to activated leukocytes, Circulation 102 (22) (2000) 2745–2750.
[7] J.R. Lindner, J. Song, J.P. Christiansen, A.L. Klibanov, F. Xu, K. Ley, Ultrasound assessment of inflammation and renal tissue injury with microbubbles targeted to P-selectin, Circulation 104 (17) (2001) 2107–2112.
[8] M. Takeuchi, K. Ogunyankin, N.G. Panian, T.P. McCreery, R.H. Sweitzer, V.E. Caldwell, E.C. Unger, E. Avelar, M. Sheahan, R. Connolly, Enhanced visualization of intravascular and left atrial appendage thrombus with the use of a thrombus-targeting ultrasonographic contrast agent (MRX-408A1): in vivo experimental echocardiographic studies, J. Am. Soc. Echocardiogr. 12 (12) (1999) 1015–1021.
[9] E.C. Unger, T.P. McCreery, R.H. Sweitzer, V.E. Caldwell, Y. Wu, Acoustically active lipospheres containing paclitaxel: a new therapeutic ultrasound contrast agent, Invest. Radiol. 33 (12) (1998) 886–892.
[10] R. Bekeredjian, S. Chen, P.A. Frenkel, P.A. Grayburn, R.V. Shohet, Ultrasound-targeted microbubble destruction can repeatedly direct highly specific plasmid expression to the heart, Circulation 108 (8) (2003) 1022–1026.
[11] S. Chen, R.V. Shohet, R. Bekeredjian, P. Frenkel, P.A. Grayburn, Optimization of ultrasound parameters for car-

diac gene delivery of adenoviral or plasmid deoxyribonucleic acid by ultrasound-targeted microbubble destruction, J. Am. Coll. Cardiol. 42 (2) (2003) 301–308.
[12] F.S. Villanueva, R.J. Jankowski, S. Klibanov, M.L. Pina, S.M. Alber, S.C. Watkins, G.H. Brandenburger, W.R. Wagner, Microbubbles targeted to intercellular adhesion molecule-1 bind to activated coronary artery endothelial cells, Circulation 98 (1) (1998) 1–5.
[13] A.L. Klibanov, M.S. Hughes, F.S. Villanueva, R.J. Jankowski, W.R. Wagner, J.K. Wojdyla, J.H. Wible, G.H. Brandenburger, Targeting and ultrasound imaging of microbubble-based contrast agents, Magn. Res. Mater. Phys., Biol. Med. 8 (3) (1999) 177–184.
[14] G.E. Weller, F.S. Villanueva, A.L. Klibanov, W.R. Wagner, Modulating targeted adhesion of an ultrasound contrast agent to dysfunctional endothelium, Ann. Biomed. Eng. 30 (8) (2002) 1012–1019.
[15] K.D. Patel, K.L. Moore, M.U. Nollert, R.P. McEver, Neutrophils use both shared and distinct mechanisms to adhere to selectins under static and flow conditions, J. Clin. Invest. 96 (4) (1995) 1887–1896.
[16] S.D. Rodgers, R.T. Camphausen, D.A. Hammer, Sialyl Lewis^x-mediated, PSGL-1-independent rolling adhesion on P-selectin, Biophys. J. 79 (2) (2000) 694–706.
[17] D.J. Goetz, D.M. Greif, H. Ding, R.T. Camphausen, S. Howes, K.M. Comess, K.R. Snapp, G.S. Kansas, F.W. Luscinskas, Isolated P-selectin glycoprotein ligand-1 dynamic adhesion to P- and E-selectin, J. Cell Biol. 137 (2) (1997) 509–519.
[18] J.E. Blackwell, N.M. Dagia, J.B. Dickerson, E.L. Berg, D.J. Goetz, Ligand coated nanosphere adhesion to E- and P-selectin under static and flow conditions, Ann. Biomed. Eng. 29 (6) (2001) 523–533.
[19] R. Bosse, D. Vestweber, Only simultaneous blocking of the L- and P-selectin completely inhibits neutrophil migration into mouse peritoneum, Eur. J. Immunol. 24 (12) (1994) 3019–3024.
[20] G.T. Hermanson, Bioconjugate Techniques, Academic Press, San Diego, CA, 1996, pp. 382–384.
[21] N.M. Green, A spectrophotometric assay for avidin and biotin based on binding of dyes by avidin, Biochem. J. 94 (1965) 23c–24c.
[22] M. Suonpaa, E. Markella, T. Stahlberg, I. Hemmila, Eu-labeled streptavidin as a universal label. Indirect time-resolved immunofluorometry of FSH and LH, J. Immunol. Methods 149 (2) (1992) 247–253.
[23] A.L. Klibanov, H. Gu, J.K. Wojdyla, J.H. Wible, D.H. Kim, D. Needham, F.S. Villanueva, G.H. Brandenburger, Attachment of ligands to gas-filled microbubbles via PEG spacer and lipid residues anchored at the interface, Proceedings of the 26th International Symposium on Controlled Release of Bioactive Materials, Controlled Release Society, Boston, MA, 1999, pp. 124–125.
[24] M.B. Lawrence, T.A. Springer, Leukocytes roll a selectin at physiologic flow rates: distinction from and prerequisite for adhesion through integrins, Cell 65 (5) (1991) 859–873.
[25] G. Thoma, J.T. Patton, J.L. Magnani, B. Ernst, R. Ohrlein, R.O. Duthaler, Versatile functionalization of polylysine: synthesis, characterization, and use of neoglycoconjugates, J. Am. Chem. Soc. 121 (25) (1999) 5919–5929.
[26] M. Takada, K.C. Nadeau, G.D. Shaw, N.L. Tilney, Prevention of late renal changes after initial ischemia/reperfusion injury by blocking early selectin binding, Transplantation 64 (11) (1997) 1520–1525.
[27] S. Ushiyama, T.M. Laue, K.L. Moore, H.P. Erickson, R.P. McEver, Structural and functional characterization of monomeric soluble P-selectin and comparison with membrane P-selectin, J. Biol. Chem. 268 (20) (1993) 15229–15237.
[28] S.C. Kuo, D.A. Lauffenburger, Relationship between receptor/ligand binding affinity and adhesion strength, Biophys. J. 65 (5) (1993) 2191–2200.
[29] E.Y. Park, M.J. Smith, E.S. Stropp, K.R. Snapp, J.A. DiVietro, W.F. Walker, D.W. Schmidtke, S.L. Diamond, M.B. Lawrence, Comparison of PSGL-1 microbead and neutrophil rolling: microvillus elongation stabilizes P-selectin bond clusters, Biophys. J. 82 (4) (2002) 1835–1847.
[30] B.T. Marshall, M. Long, J.W. Piper, T. Yago, R.P. McEver, C. Zhu, Direct observation of catch bonds involving cell-adhesion molecules, Nature 423 (6936) (2003) 190–193.
[31] K. Ley, P. Gaehtgens, Endothelial, not hemodynamic, differences are responsible for preferential leukocyte rolling in rat mesenteric venules, Circ. Res. 69 (4) (1991) 1034–1041.
[32] D.L. Elbert, J.L. Hubbell, Surface treatments of polymers for biocompatibility, Annu. Rev. Mater. Sci. 26 (1996) 365–394.
[33] T. Jossang, J. Feder, E. Rosenqvist, Photon correlation spectroscopy of human IgG, J. Protein Chem. 7 (2) (1988) 165–171.
[34] M.W. Keller, S.S. Segal, S. Kaul, B. Duling, The behavior of sonicated albumin microbubbles within the microcirculation: a basis for their use during myocardial contrast echocardiography, Circ. Res. 65 (2) (1989) 458–467.